About the Free Surface Flow Simulation around a TLP

M. Goodarzi[1], A. Yalpaniyan[2]

[1,2]Bu-Ali Sina University, Hamedan, Iran

[1]m.goodarzi@basu.ac.ir; [2]a.yalpanian@basu.ac.ir

Abstract

The TLP of interest in this study is a buoyant platform with four piers and pantoons. The purpose of this study was to consider the effects of applying different solvers in the numerical simulation on the prediction of the flow pattern around the TLP. The flow around the TLP was numerically simulated with inviscid, laminar, and turbulent solvers. Each case were performed for three different Froude Numbers. To simplify the calculations symmetry condition was considered. Besides the generated surface waves there was a pair of non-symmetrical vortexes after each pier. The vortex after the front pier significantly affected the flow pattern around the rear one in the manner that the vortex behind the rear pier was clearly smaller. In all cases the vortex more distanced from the symmetry plane was larger than the closer one. The obtained results showed that the generated waves resulting from inviscid solver were smoother than those of the turbulent and laminar solvers accordingly. Finally, it was concluded that the effect employing turbulent or laminar solver was negligible compared to the effects of different Froude numbers.

Keywords

Flow Pattern; VOF; TLP; Vortex; Free Surface

Introduction

Marine Science is an established branch of Fluid Mechanics which has been studied for several years in both academic and practical methods. Marine structures and buoyant platforms are subjects of great interest in this branch. Piers and Tension Leg Platforms (TLP) has drawn much attention and were studied from different points of view. In recent decades many studies were carried out about TLPs. Most of them were based on the vibration response due to the regular and irregular incident waves by simplifying the real model with a simple vibration model. Some of these studies were mentioned here. Sai Baba et al (1998) developed a computer package for designing the piles under cyclic tensile load. Adrezin and Benaroya (1999) studied the response of a tension leg platform to stochastic wave forces. Niedzwecki et al (2000) used experimental data to study surface wave interaction with compliant deepwater platforms. Muhittin and Yılmaz (2003) considered hydrodynamic forces in design of a TLP type off-loading platform. The effect of second-order perturbation added mass fluctuation on vertical vibration of a tension leg platform was also considered by Tabeshpour et al (2006). Low (2009) used statistical linearization of the tendon restoring forces for analysis of a tension leg platform. In a few number of studies, free surface flow around platform was considered in numerical modeling. For example, Younis and Przulj (2006) predicted the hydrodynamic loading on a mini TLP with inserting the free-surface effects in the numerical procedure. They had also studied hydrodynamic forces on a mini TLP with computational fluid dynamics and design-code techniques without considering the free surface (Younis et al 2001) before. It was worth mentioning that in the recent work of Younis and Przulj (2006), the separation flow behind the piers was not predicted; which was not physically possible in a viscose flow. James et al (2002) used a surface tracking method for hull component interaction and scaling for TLP hydrodynamic coefficients.

In the present work a surface capturing method was used to predict the flow field around a TLP for different cases. Different Froude numbers for laminar and turbulent flow regimes was considered (Fr = 0.12, 0.18, 0.24). The speeds registered for surface currents were almost around 2.5 m/s which based on our formulation for Froude number gave a Froude number around 0.15, so the three mentioned Froude numbers were chosen to cover a majority of the critical current speeds. The numerical method used in this study was Volume of Fluid (VOF) (Hirt and Nicholas 1981).

Materials and Methods

To study the flow pattern and effects of flow regime presumptions, continuum and momentum equations were considered as governing equations of flow for both phases of water and air. In addition, a

transmission equation was used to determine the volume fraction (Hirt and Nicholas 1981) of either phase in each cell of the calculation domain. These calculations were performed with SIMPLE algorithm (Patankar 1980) in so called commercial software, FLUENT. These equations were simplified for incompressible flow as follows:

$$\frac{\partial U_i}{\partial x_i} = 0 \tag{1}$$

$$\frac{\partial U_i}{\partial \tau} + U_j \frac{\partial U_i}{\partial x_j} = \frac{\partial}{\partial x_j}\left(\upsilon \frac{\partial U_i}{\partial x_j} - \overline{u_i u_j} \right) - \frac{1}{\rho}\frac{\partial p}{\partial x_i} \tag{2}$$

$$\frac{\partial c}{\partial t} + div(cv) = 0 \tag{3}$$

RNG (Re-Normalized Group) type of (k-ε) (Launder and Spalding 1972) turbulence model was used for turbulent solver. This model has been used by many researchers for free surface flows which have complex turbulent patterns. The algorithms and methods mentioned above were well known so, for concision, they were not expanded here. In case, they were explained thoroughly in references.

To solve the governing equations, it is important to define the boundary conditions properly. The boundary condition used at the solid boundaries was physical defined as no-sliding condition. In the domain of air phase the pressure was assumed to be consistent and equal to the atmospheric pressure, a little different from the reality. As it has been assumed in former studies performed in this field, considering this condition's effect on the results obtained in the liquid phase was negligible, its precision for our calculations was acceptable. A case study was used to define an optimized grid number in which the numerical results were not dependent on mesh system.

Results and Discussions

The precision and accuracy of software were determined by solving a 2D free surface model for which the experimental data were available. As it is illustrated in figure 1 this case is a 2D model of water flow over a semicircular bump. Figure 1 also shows the mesh used for this model. Model's dimensions are defined in proportion to the bump's diameter. The height and length of meshed domain are respectively 1.6 and 20 times of semicircle's diameter. The length considered after the bump is about 9 times the semicircle's diameter. According to the experimental model used by Forbes (1988) the referenced diameter is 3 cm.

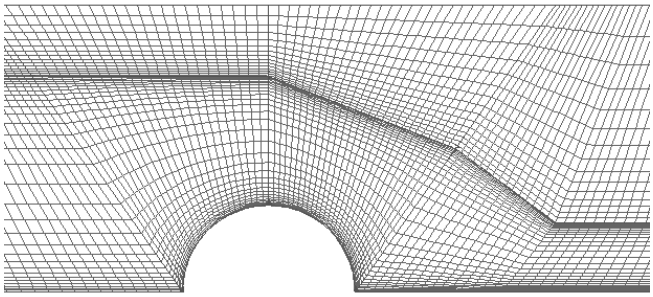

FIGURE 1 GRID STRUCTURE OF 2D MODEL

Flow stream lines over the bump for the Froude number of 0.336 and a constant fraction of radius to the height of upper hand flow (R/H=0.435) are shown in figure 2. As figure 2 shows in addition to loss in flow's height, there is a separation behind the bump which is a characteristic of viscous flows. Separation area is smaller than what could be seen in absence of free surface condition. The reason for this event can be explained by considering the reduction of static pressure due to loss of height after the bump and increase in velocity, again, because of the height loss. All of these are consequences of considering free surface flow.

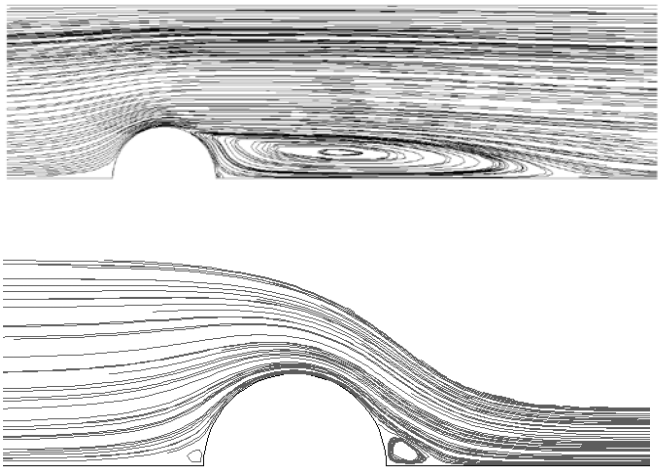

FIGURE 2 STREAM LINES OF A SIMPLE AND A FREE SURFACE 2D FLOW OVER A BUMP

Figure 3 shows free surface level of flow over the bump measured by Forbes (1988) and free surface level resulted in the present numerical study. This comparison shows a good agreement between the present numerical results and experimental results.

After determining the reliability of this method for free surface flow, we simulated a 3D model of flow around a TLP. Figure 4 shows a symmetric half of this model. Because of the symmetric shape of flow and TLP we

only studied one half of actual model. The mesh structure of this model is also illustrated in figure 4. This model is prepared by the actual dimensions listed in table 1. In this model, governing equations are solved for Inviscid, laminar and turbulent regimes. For each case, three different Froude numbers are run. The free surface level is assumed to be about 57.25m in entrance of the model for all cases. The distance between entrance and exit is about 150m. Froude number is calculated by following equation:

$$Fr = \frac{U}{\sqrt{g(H+B)}} \quad (4)$$

In this equation U, g, H, and B respectively denote the flow velocity, gravitational acceleration, the pier height, and the Pontoon height.

Free surface profile around the piles is illustrated in figure 5 for laminar and turbulent flow regimes. In each case the free surface profile is presented for three different Froude numbers. We can see that the general form of the free surface profile is about the same for all Froude numbers and it is not strongly dependant to the Froude number. The noticeable point is the variation of difference between the extreme levels of the free surface which here is called Amplitude (table 2). Though these amplitudes vary significantly by Froude numbers but they are almost the same for both flow regimes as well as surface profiles. Results show the wave generated amplitudes raise with the increase of Froude number. Another interesting point is the mentioned similarity of free surface profile for laminar and turbulent regime in every Froude number. This similarity can be discussed in two ways. In the study of free surface flow the differences between the results for laminar and turbulent regimes in large scales are not considerable, because of the complexity of the flow pattern, in other words, the flow pattern is too complicated for turbulence characteristics to grow. Due to the fact that the size of smallest elements in a grid structure for a model with real dimensions is considerably large, turbulence length scales are too small to be traced in the flow. So the loss of their effects on the flow is inevitable. It is obvious in figure 5 and figure 6 that the small differences between surface profiles of laminar and turbulent regimes have increased by the raise of Froude number though they are still insignificant. This is due to the increase of turbulence velocity scales and, consequently, enlargement of turbulence length scales which could be caught partly by this large grid structure. This penetration of turbulence effects in the flow decreases the amplitude of the generated waves. The difference between laminar and turbulent flow regimes is more obvious in table 2 which contains amplitudes of the free surface profiles.

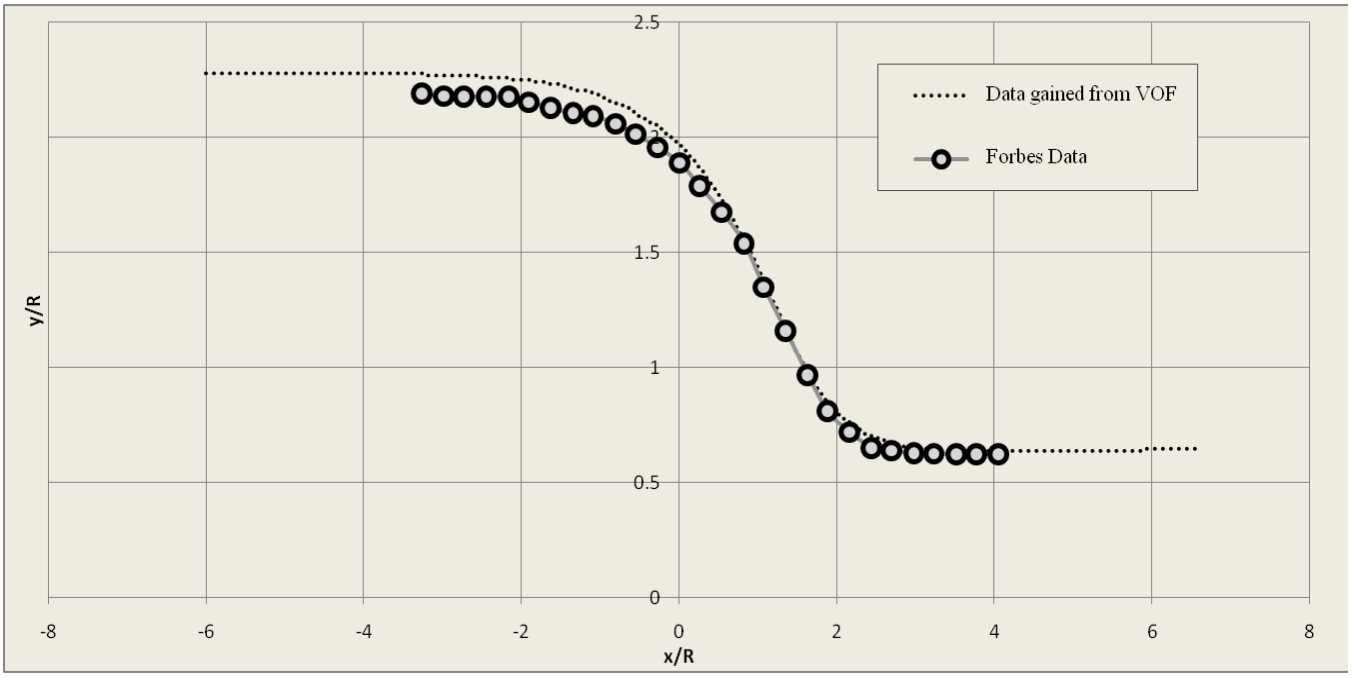

FIGURE 3 COMPARISON BETWEEN PRESENT NUMERICAL RESULTS AND EXPERIMENTAL DATA OF FORBES FOR FR=0.336 AND R/H=0.435

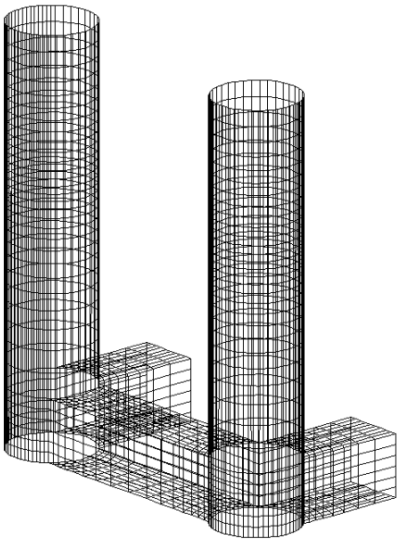

FIGURE 4 GRID STRUCTURE OF TLP MODEL

TABLE 1 DIMENSIONS OF TLP MODEL

Part	Dimension (m)
Pier diameter	8.75
Pier's in water height	22.25
Distance between two piers	28.5
Pontoon's height	6.25
Pontoon's width	6.25
Draft	28.5

TABLE 2 AMPLITUDES OF SURFACE PROFILES IN METERS (M)

Fr	0.12	0.18	0.24
Laminar flow	*1.45*	*3.32*	*8.19*
Turbulent flow	*1.43*	*3.23*	*7.0*

Stream lines at the free surface show a couple of vortexes behind each pier. Vortexes made behind the first pier lead the flow someway that the vortexes behind the second pier are smaller than what supposed to be if there was only one pier (Figure 6). It's like putting a pier in a converging channel so that the stream lines coming toward this pier somehow would meet somewhere after the pier. As it is suspected, since these vortexes root from velocity gradient and velocity profile inflection, this occurrence is more apparent in large Froude numbers. According to figure 6 the size of these vortexes has a rather direct relation to free surface profile amplitudes. This pattern proportionately goes for other sections of flow, like; vertical sections, as well. A sample of stream lines on symmetry plane is shown if figure 7 for Fr=0.18.

Based on velocity vectors shown in figure 8 for inviscid, laminar and turbulent flow with Fr=0.18, it can be seen that the size of vortexes in inviscid flow are considerably smaller than those of laminar and turbulent flows while vertex sizes for those two latter flows are almost the same. So, it can be concluded that the laminar regime assumption for smaller Froude numbers gives an acceptable prediction of flow pattern compared to the turbulent flow assumption but the prediction of the inviscid flow assumption is rather unrealistic.

Conclusion

Full scale computation of a large dimension platform concerns with large control volumes in the numerical procedure. Therefore in numerical computation for small Froude numbers, small scales cannot be captured to precisely predict turbulent behaviors. As the Froude number increases, these length scales will be enlarged such that numerical computation can overcome the mentioned physical discrepancy and predict the encountered turbulent flow in details due to larger turbulence scales. Hence, it is possible to neglect the turbulence characteristics in numerical computation for small Froude numbers.

References

Adams, John, et al. "Ocean Currents." *Microsoft Encarta*. 2 vols. CD-ROM. Redmond: Microsoft, 1999. 191.

Adrezin, R., Benaroya, H., Response of a tension leg platform to stochastic wave forces, Probabilistic Engineering Mechanics 14 (1999) 3-17. 1999.

Coble, Charles R., Elaine G. Murray, and Dale R. Rice. *Earth Science*. 3rd ed. Englewood Cliffs, NJ: Prentice Hall, 1987: 256-257.

Forbes, L.K., Critical free-surface flow over a semi-circular obstruction. J. Eng. Math. 2, 3-13. 1988.

Gaskell, T F. *The Gulf Stream*. New York: John Day Company, 1973. 95.

Gross, M.G., *Oceanography: A View of the Earth*. 3rd ed. New York: Prentice Hall, 1982: 173, 177.

Gross, M G. *Oceanography*. 6th ed. Columbus: Merrill, 1990: 74-75.

Hirt, C.W., Nicholas, B.D., Volume of Fluid (VOF) Method for the Dynamics of Free Boundaries, J. Computational Physics, 39: pp. 201- 225. 1981.

James, J. O'Kane, et al, Hull component interaction and scaling for TLP hydrodynamic coefficients, cean Engineering 29, 513–532. 2002.

Launder, B.E., Spalding, D.B., Mathematical Models of Turbulence, Academic press, London & New York; 1972.

Low, Y.M., Frequency domain analysis of a tension leg platform with statistical linearization of the tendon restoring forces, Marine Structures 22, 480–503. 2009.

Muhittin Soylemez, Oguz Yılmaz, Hydrodynamic design of a TLP type offloading platform, Ocean Engineering 30, 1269–1282. 2003.

Niedzwecki, J.M., et al, Design estimates of surface wave interaction with compliant deepwater platforms, Ocean Engineering 27, 867–888. 2000.

Patankar, S., Numerical Heat Transfer and Fluid Flow, Hemisphere publishing corporation, McGraw Hill Book Co., New York. 1980.

Sai Baba Reddy E., O'Reilly, M., Chapman, D.N., A computer package for the design of piles under cyclic tensile load, Computers and Structures 69,149-158. 1998.

Tabeshpour, M.R., Golafshani, A.A., Seif, M.S., Second-order perturbation added mass fluctuation on vertical vibration of tension leg platforms, Marine Structures 19, 271–283. 2006.

Younis, B.A., Teigen, P., Przulj, V.P., Estimating the hydrodynamic forces on a mini TLP with computational fluid dynamics and design-code techniques, Ocean Engineering 28, 585–602. 2001.

Younis, B.A., Przulj, V.P., Prediction of hydrodynamic loading on a mini TLP with free-surface effects, Ocean Engineering 33, 181-204. 2006.

Fr	Laminar flow	Turbulent flow
0.12	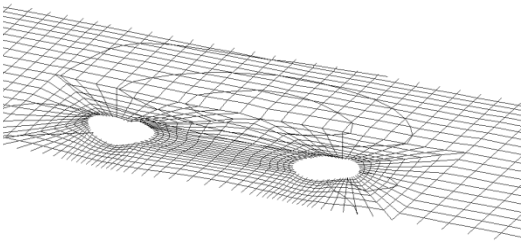	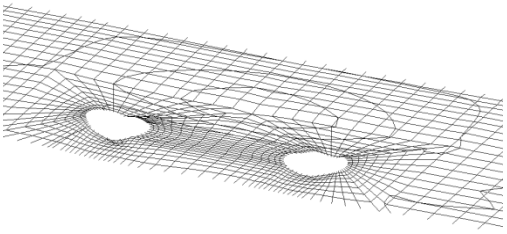
0.18	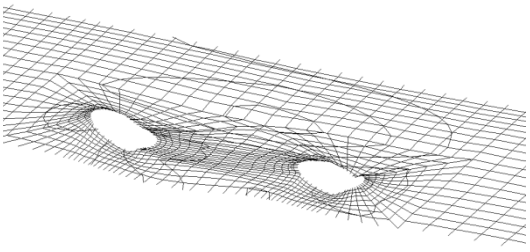	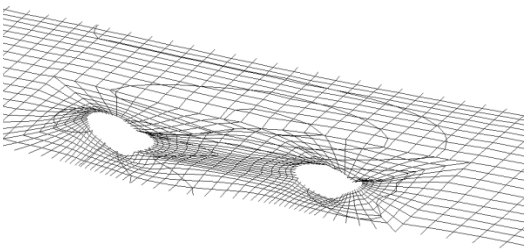
0.24	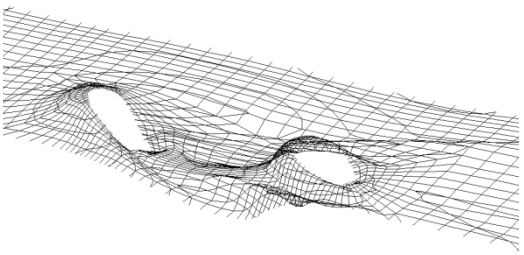	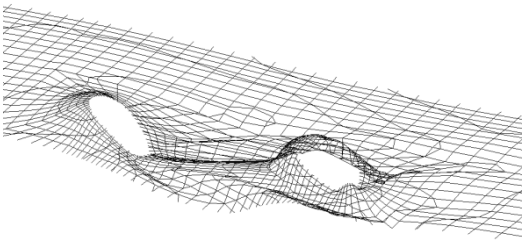

FIGURE 5 FREE SURFACE PROFILE FOR LAMINAR AND TURBULENT REGIMES

Fr	Laminar flow	Turbulent flow
0.12	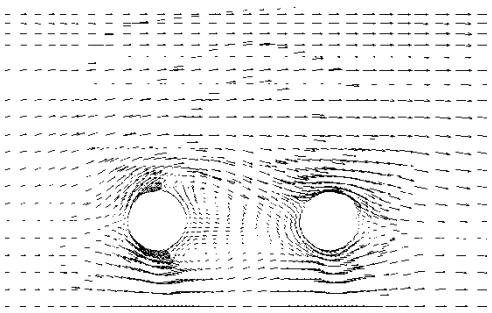	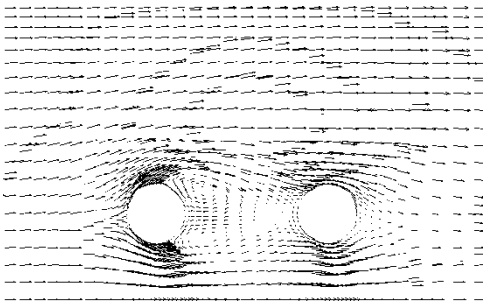
0.18	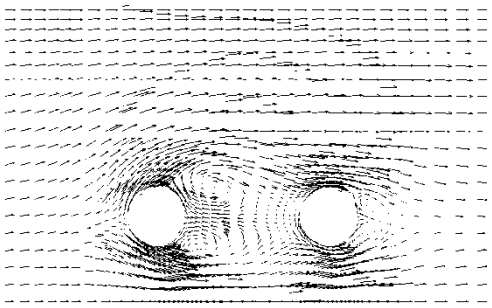	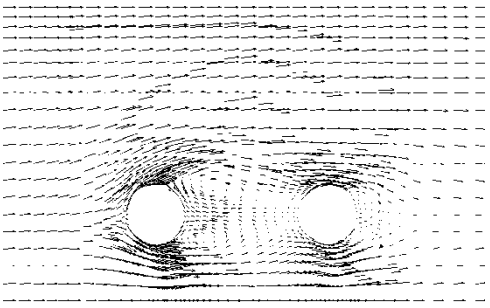
0.24	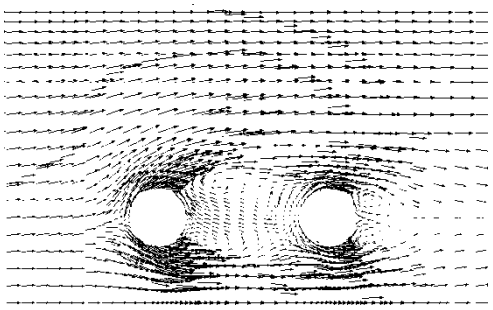	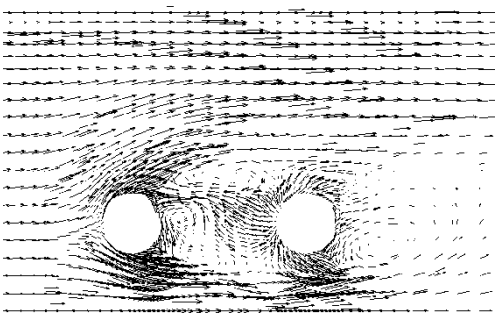

FIGURE 6 VELOCITY VECTORS ON THE CLOSEST PLANE TO THE FREE SURFACE FOR LAMINAR AND TURBULENT REGIMES

Laminar flow	Turbulent flow
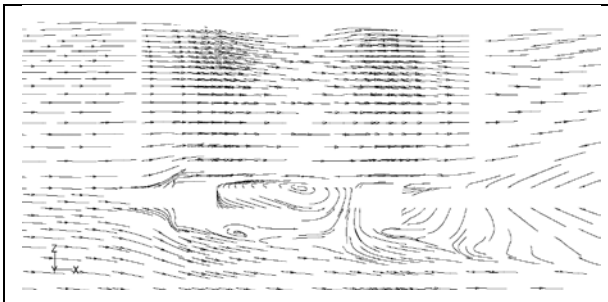	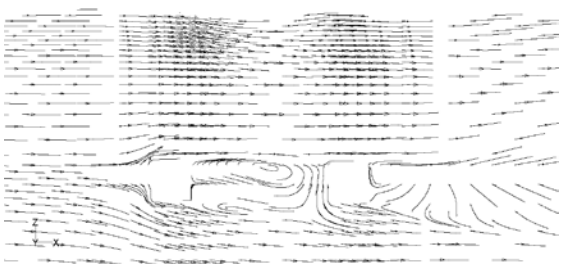

FIGURE 7 STREAM LINES ON SYMMETRY PLANE FOR FR=0.18

Flow Regime	Fr = 0.18
Inviscid	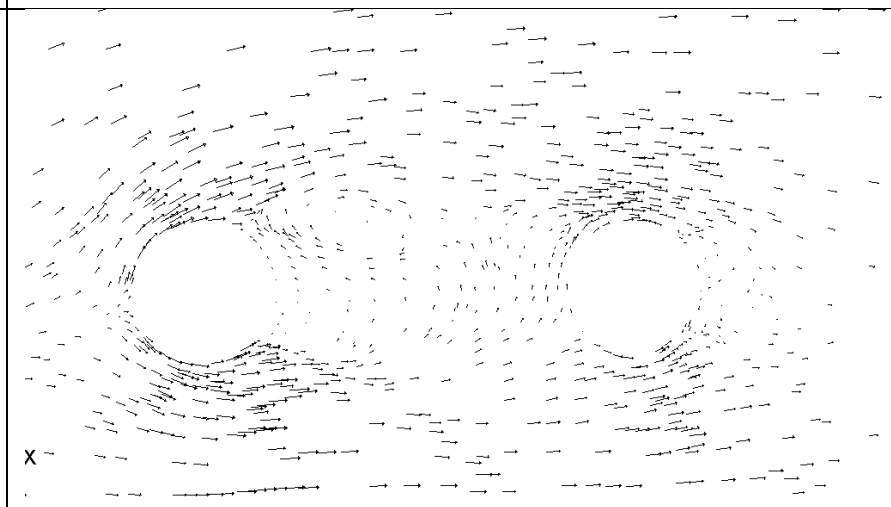
Laminar	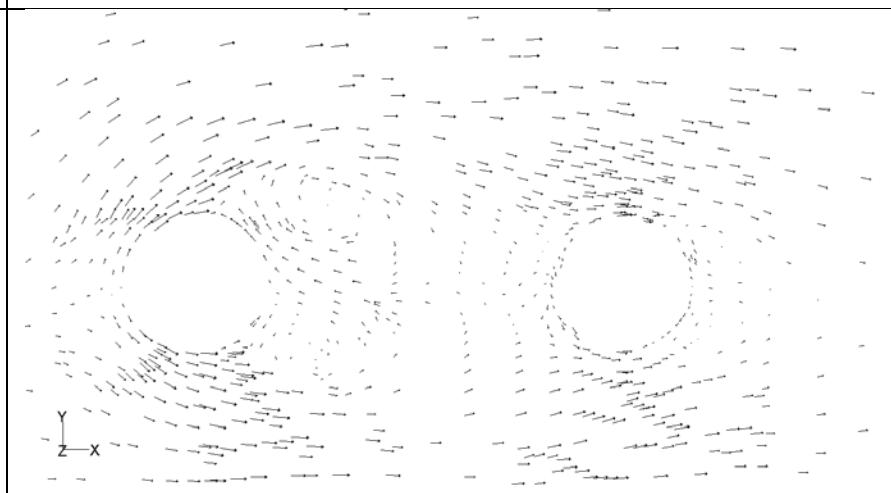
Turbulent	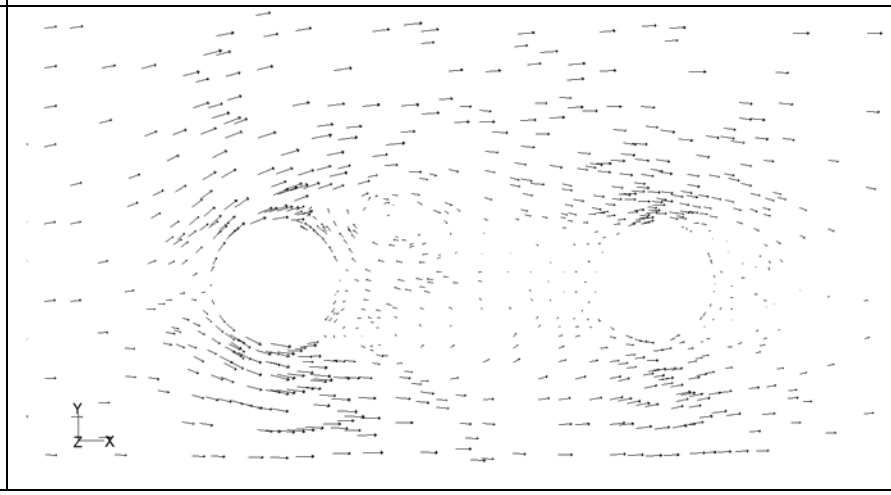

FIGURE 8: VELOCITY VECTORS ON THE CLOSEST PLANE TO THE FREE SURFACE FOR FR = 0.18